# Novel Photophysical Properties of Gold Selenide Complexes: Photogeneration of Singlet Oxygen by $[Au_{18}Se_8(dppe)_6]Br_2$ and Near-Infrared Photoluminescence of $[Au_{10}Se_4(dpppe)_4]Br_2$

**Sergei Lebedkin,*,†,‡ Timo Langetepe,§ Paloma Sevillano,§ Dieter Fenske,†,§ and Manfred M. Kappes†,‡**

*Forschungszentrum Karlsruhe, Institut für Nanotechnologie, D-76021 Karlsruhe, Germany, Institut für Physikalische Chemie II, Universität Karlsruhe, D-76128 Karlsruhe, Germany, and Institut für Anorganische Chemie, Universität Karlsruhe, D-76128 Karlsruhe, Germany*

*Received: May 1, 2002*

The photoluminescence (PL) properties of several recently synthesized ligand-stabilized polynuclear gold(I) selenide complexes were investigated. $[Au_{18}Se_8(dppe)_6]Br_2$ {dppe = bis(diphenylphosphanyl) ethane} (**I**) is distinguished by the bright-red long-lived PL (phosphorescence) in the solid state, photosensitization of singlet oxygen, $^1O_2$, in solution, and high photostability. The quantum yield of PL, $\varphi_{PL}$, is $(7.5 \pm 0.5) \times 10^{-2}$ for the polycrystalline **I** at 293 K (determined using an integrating sphere) and increases up to ∼0.8 at 77 K. The quantum yield of $^1O_2$ is $0.17 \pm 0.02$ in $O_2$-saturated dichloromethane solutions. $[Au_{10}Se_4(dpppe)_4]Br_2$ {dpppe = bis(diphenylphosphanyl)pentane} (**II**) shows a broad near-infrared PL at 880 nm in dichloromethane [$\varphi_{PL} = (4 \pm 1) \times 10^{-3}$], which is shifted up to ∼1020 nm in the solid **II** at 77 K ($\varphi_{PL} \sim 3 \times 10^{-3}$). Although the quantum efficiency of **II** as a luminophor is quite moderate, it is comparable to that of organic infrared laser dyes such as Styryl-20 and IR26. A particular configuration of the $Au_{10}Se_4$ core appears to be crucial for the near-infrared PL: the "isomeric" complexes $[Au_{10}Se_4(dppm)_4]Br_2$ {dppm = bis(diphenylphosphanyl) methane} (**III**) and $[Au_{10}Se_4(depe)_4]Cl_2$ {depe = bis(diethylphosphanyl) ethane} (**IV**) show no significant PL.

## 1. Introduction

Photophysical properties of nanoscale objects are of interest both for fundamental reasons as well as for applications in areas ranging from optoelectronics to chemical/biological sensors.[1] In recent years activities in this field have been driven primarily by the availability of well characterized materials—with particular developments along the sequence polydispersed → monodispersed/single nanocrystals/clusters for the substance classes cadmium selenide/sulfide[2] and ligand-stabilized gold.[3] In the case of cadmium selenide, much interest was attracted by the remarkably high photoluminescence (PL) quantum yields observed in nanometer particles.[4] These show a strong size dependence of optical absorption and emission maximum, with smaller particles generally having shorter wavelength absorption and emission.[5] In an effort to characterize the small particle limit, it has recently proven possible to synthesize a set of ligand-stabilized cadmium selenide cluster complexes and to study their PL properties.[6] It has been shown that the absorption and emission maxima of the clusters as small as $Cd_8Se_{11}$ and $Cd_4Se_6$ follow the above trend, but other photophysical properties such as PL kinetics and photostability depend on many factors and cannot be correlated only to the cluster size.[6]

There have been only a few reports about relatively weak luminescence of nanometer-size gold particles.[7−9] On the other hand, ligand-stabilized gold(I) complexes with one or a few gold atoms show remarkably rich photophysical and photochemical behavior reflecting the diversity of their structures.[10] Characteristic for many of them is a bright visible PL with a large Stokes shift and a slow microsecond decay. The luminescence is often very sensitive to the complex configuration and molecular surroundings and this may be used for chemical sensor applications.[11,12] The changes of PL can be related to the corresponding changes of intra/intermolecular gold−gold interactions. In ligated complexes comprising several formally cationic gold atoms, Au···Au nearest neighbor separations are often surprisingly short (∼2.9−3.4 Å). While still somewhat longer than in the metallic gold solid (nearest neighbor separation 2.88 Å)[13] or in small bare $Au_n^+$ clusters (2.82 Å average bond distance for $n = 13$)[14] these separations are definitely sub-van der Waals. Short Au···Au contacts and the associated gold−gold interactions (the phenomenon of aurophilicity[15]) are thought to play an important role for the photophysical properties of such systems, as has been well demonstrated for a number of di-, tri-, and tetranuclear gold compounds.[11,12,16−18] From this point of view, studies of still larger, cluster-like structures with many (interacting) gold atoms are of particular interest. Among their useful properties could also be a large absorption cross-section, i.e., an efficient photoexcitation, as well as a relatively high photostability. An established synthetic route to such complexes, which has been actively developed in the last years, takes advantage of chalcogenides, typically sulfur or selenium, to bridge gold(I) atoms in a core and of suitable ligands, typically phosphines, to stabilize the whole structure. Still, relatively few large polynuclear gold complexes have been synthesized and structurally characterized so far. Examples include complexes with the $Au_{12}S_4$ and $Au_{10}S_4$ cores,[19] which were found to be luminescent.

In this work, we have investigated the photophysical properties of recently synthesized polynuclear gold(I) selenide complexes with the $Au_{18}Se_8$ and $Au_{10}Se_4$ cores.[20,21] Their crystal structures (**I**−**IV**) are shown in Figure 1. Multiple gold−gold

* Corresponding author. Fax: +49 7247 826368. E-mail: lebedkin@int.fzk.de;
† Institut für Nanotechnologie.
‡ Institut für Physikalische Chemie.
§ Institut für Anorganische Chemie.

10.1021/jp021100p CCC: $22.00 
Published on Web 08/08/2002

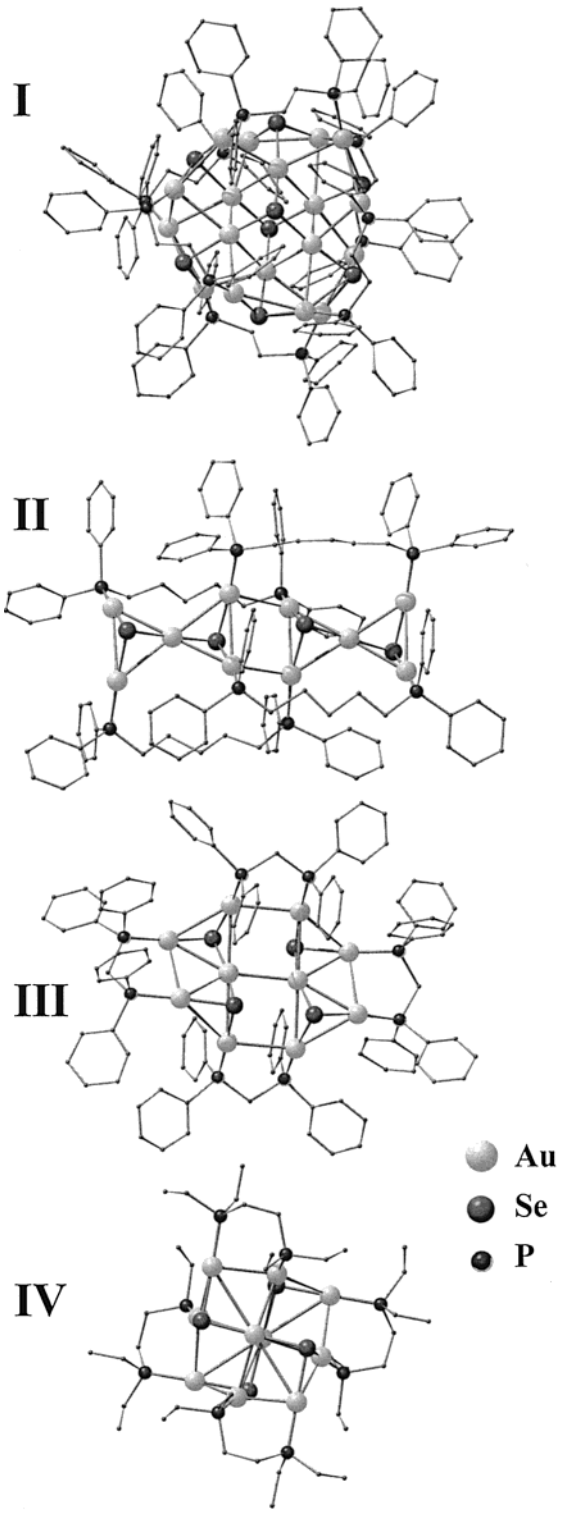


**Figure 1.** X-ray crystal structures of the gold selenide complexes studied in this work. **I**: $[Au_{18}Se_8(dppe)_6]Br_2$, dppe = bis(diphenylphosphanyl)ethane; **II**: $[Au_{10}Se_4(dpppe)_4]Br_2$ {dpppe = bis(diphenylphosphanyl)pentane}; **III**: $[Au_{10}Se_4(dppm)_4]Br_2$, {dppm = bis(diphenylphosphanyl) methane}; **IV**: $[Au_{10}Se_4(depe)_4]Cl_2$ {depe = bis(diethylphosphanyl)ethane}. Hydrogen atoms and counteranions are not shown for clarity. The Au−Au contacts are 2.94−3.33 Å in **I**, 2.98−3.35 Å in **II**, 3.03−3.36 Å in **III**, and 2.99−3.27 Å in **IV** (refs 20, 21).

contacts (interactions) are characteristic for all these structures. The complex **I** has also attracted our attention because of its peculiar "multishell" $Au_{18}Se_8$ core, bright-red photoluminescence seen by the naked eye, and high chemical stability. We found that another remarkable property of **I** is its effective photosensitization of singlet oxygen in solution. The $Au_{10}Se_4$ complexes **II**−**IV** represent a series of compounds with different "isomeric" gold selenide cores, and a comparison of their properties is of particular interest. Among these complexes, only **II** was found to be luminescent with a moderate quantum yield under UV−visible irradiation. A remarkable feature of the PL of **II** is its low emission energy (near-infrared luminescence) and, correspondingly, very large Stokes shift. To our knowledge, these are the first observations of near-infrared PL and effective photosensitization of singlet oxygen for ligand-stabilized gold complexes. We also describe a procedure for determination of photoluminescence quantum yields of powdered samples using an integrating sphere and a conventional luminescence spectrometer.

## 2. Experimental Details

**2.1. Materials.** The synthesis and crystallographic analysis of the gold selenide complexes **I**, **III** have been reported previously.[20] The corresponding data for **II**, **IV** are presented elsewhere.[21] On the basis of crystal structures the formal oxidation state of all gold atoms in **I**−**IV** was assigned as Au(I). Briefly, **I**−**IV** were prepared by the exchange reaction of $[(AuBr)_2L]$ or $[(AuCl)_2L]$, where L is a corresponding ligand, with $Se(SiMe_3)_2$ [*n*-$BuSe(SiMe_3)$ for **IV**] in dichloromethane at room temperature using standard Schlenk techniques. The similar reaction conditions indicate that the ligands are of a prime importance for the size and structure of a gold selenide core in the product. After crystallization out of solution, the orange-red powder of **I** and yellow powders of **II**−**IV** were either redissolved in dichloromethane or stored as solids. Laser dyes Coumarin 307 (LC5000), Rhodamines 6G, B, and 800 (LC8000), Styryl 20 (LC9940), and IR26 (LC1080) were obtained from Lambda Physik; solvents (analytical grade) were obtained from Merck; these chemicals were used as received. $C_{70}$ was prepared and chromatographically purified (>99%) in our lab.

**2.2. Absorption and Photoluminescence Measurements.** UV−visible spectra were recorded on a Perkin-Elmer Lambda 900 spectrophotometer. PL measurements were performed on a Spex Fluorolog-3 spectrometer equipped with a 450 W Xe-lamp and double-grating monochromators in the excitation ($\lambda_{exc}$ ~250−1000 nm) and two emission channels. Three photodetectors—R928 and R5108 Hamamatsu photomultiplier tubes (PMT) and a liquid nitrogen-cooled germanium photodiode (Edinburgh Instruments)—covered the emission ranges of $\lambda_{em}$ ~ 300−850 (UV−visible emission channel), ~ 680−1150, and ~ 900−1700 nm (NIR emission channel), respectively. Near-infrared PL spectra were typically combined from the curves obtained with both NIR detectors. All emission spectra were corrected for the wavelength-dependent instrumental response. The latter was determined using a standard calibration lamp (Oriel) and a two-inch Spectralon integrating sphere (Labsphere) installed in the sample chamber of the Fluorolog-3 spectrometer.

Time-resolved luminescence was recorded with the R5108 PMT connected to a LeCroy LT322 Waverunner oscilloscope (50 Ω load). A $N_2$-laser (337 nm, ≤4 ns, ~20 μJ) was used for a pulse excitation. About 100−300 transients were typically accumulated in the standard acquisition mode of the oscilloscope (5 ns/point) and up to several thousands in the random interleaved sampling (RIS) mode with the effective dwell time of 100 ps/ point. In the latter case, a fast rise/decay of PL could be recorded with a time resolution of ~0.5 ns determined mainly by the stability of the laser, photodiode trigger, and PMT response. No photodecomposition of the studied gold selenide

complexes was observed during the steadystate as well as time-resolved PL measurements. To study the effect of dissolved oxygen on the PL kinetics and quantum yield, solutions were purged for ~20 min either with argon or oxygen.

**2.3. Photoluminescence Quantum Yields in Solution.** For the complexes **I** and **II** in solution, $\varphi_{PL}$ was determined at $\lambda_{exc}$ = 400 nm relative to the fluorescence quantum yield of Coumarin 307 in methanol ($\lambda_{em}$ = 497 nm, $\varphi_{fluor}$ = 0.95 ± 0.02). Coumarin 307 was itself calibrated against Rhodamine 6G in methanol ($\lambda_{em}$ = 553 nm, the value of $\varphi_{fluor}$ was taken as 0.95).[22] The quantum efficiency of the near-infrared PL of **II** was obtained from a comparison with the phosphorescence of singlet oxygen $^1O_2$ in toluene ($\lambda_{em}$ = 1275 nm, $\varphi_{phos} = 4.3 \times 10^{-6}$)[23] photosensitized by $C_{70}$ having a quantum yield $\varphi(^1O_2) \approx 1$,[24] both excited at $\lambda_{exc}$ = 400 nm. $C_{70}$ was also used as a reference sensitizer to evaluate the efficiency of photogeneration of $^1O_2$ by complex **I**. These measurements were performed using standard 10 mm cuvettes in a 90°-geometry. The refractivity effects were neglected.

**2.4. Photoluminescence Quantum Yields of Powders.** To determine $\varphi_{PL}$ of solid (powdered) samples of **I** and **II**, we employed the Spectralon integrating sphere as shown in Figure 2a. To "switch" between the two emission channels (UV−visible or NIR) of the Fluorolog-3 spectrometer, a Spectralon plug was inserted into a corresponding porthole (opposite to the channel entrance) of the sphere. Glass capillaries (1 mm i.d.) were used as sample holders (Figure 2a). As the quantum yield references for powders of **I** and **II**, we employed capillaries with concentrated solutions of, respectively, Coumarin 307 in methanol and $C_{70}$ in toluene. Because of the large Stokes shifts, reabsorption of luminescence in the samples and reference solutions could be neglected. The value of $\varphi_{PL}$ was calculated as

$$\varphi_{PL} = \varphi_{ref} \times (\Delta_{ref}/\Delta_{sample}) \times [\int PL_{sample}(\lambda)\, d\lambda / \int PL_{ref}(\lambda)\, d\lambda] \quad (1)$$

where $\varphi_{ref}$ is the reference quantum yield, $PL_{sample}$ ($PL_{ref}$) and $\Delta_{sample}$ ($\Delta_{ref}$) are corrected luminescence intensities and relative amounts of the absorbed excitation light for a sample (reference), respectively. The values of $\Delta_{sample}$ and $\Delta_{ref}$ were determined from the intensities of light scattered from the integrating sphere at the excitation wavelength $\lambda_{exc}$ (attenuated with a neutral Schott glass filter) with respect to the empty glass capillary (Figure 2b). Compared to the other methods for measuring luminescence quantum yields of powders,[25] our procedure does not require assumptions about the angular distribution of emitted light (by virtue of an integrating sphere), employs fluorophor solutions as reliable quantum yield references, and is particularly practical for small sample amounts (much less than 1 mg can be measured when diluted with KBr or another suitable powder). One should remark that under UV irradiation Spectralon fluoropolymer shows a moderate background PL with a broad maximum at ~440 nm, which tails up to ~600 nm. Therefore, the use of a Spectralon integrating sphere is limited in this range to relatively strong luminophores.

It follows from Figure 2b that the relative absorption $\Delta_{ref}$ as well as $\Delta_{sample}$ should not be too small, otherwise this would be subject to large uncertainties. Therefore, rather concentrated solutions of Coumarin 307 and $C_{70}$ [$OD(\lambda_{exc})$ ~5−10] were used in order to get a sufficient light absorption in the glass capillaries. To correct for a possible concentration dependence of the quantum yields of the fluorescence of Coumarin 307 and phosphorescence of $^1O_2$ sensitized by $C_{70}$, a separate measurement has been performed as shown in Figure 2c. For this, solutions with different concentrations of Coumarin 307 and $C_{70}$ were irradiated in a thin (1 mm) cuvette positioned off-center in the sample chamber of the Fluorolog-3 (the excitation focusing mirror was correspondingly adjusted); the fluorescence/$^1O_2$-phosphorescence was indirectly collected from a diffuse reflecting plate (Spectralon or MgO-covered aluminum); and the detector signal was compared to the fraction of the absorbed excitation light calculated from the absorption spectrum. We found that $\varphi_{fluor}$ of Coumarin 307 in methanol and $\varphi_{PL} = [\varphi(^1O_2) \times \varphi_{phos}]$ for $^1O_2$ sensitized by $C_{70}$ in toluene were practically constant within experimental error (±10%) in the concentration ranges from $\sim 10^{-5}$ up to $1.5 \times 10^{-3}$ $M^{-1}$ ($OD^{400}$ = 27) and $6.4 \times 10^{-4}$ $M^{-1}$ ($OD^{400}$ = 9.4; $OD^{470}$ = 12.4), respectively.

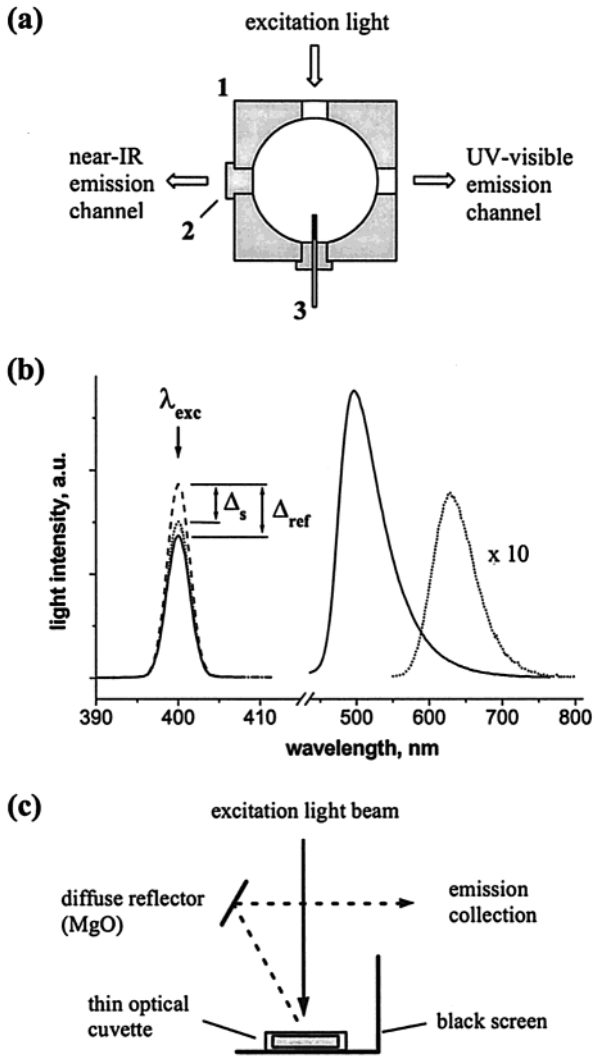


**Figure 2.** Determination of photoluminescence quantum yield of powdered samples at ambient temperature using an integrating sphere and a conventional luminescence spectrometer. (a) Schematic setup (top view) showing (**1**) Spectralon integrating sphere with four port holes in a sample chamber of a Spex Fluorolog-3 spectrometer; (**2**) removable Spectralon port plug; and (**3**) glass capillary with a sample or a reference compound/solution. (b) Photoluminescence of the polycrystalline $Au_{18}Se_8$ complex **I** (dotted line) vs fluorescence of Coumarin 307 in methanol (solid line) used as a reference. Relative absorptions of the excitation light by the sample ($\Delta_s$) and reference ($\Delta_{ref}$) are determined from the intensities of light scattered from the sphere at the excitation wavelength, $\lambda_{exc}$, (attenuated with a neutral Schott filter) with respect to the empty glass capillary (dashed line). (c) Schematic setup (top view) for measurements of a fluorescence quantum yield concentration dependence for the reference fluorophor solutions (for details see text).

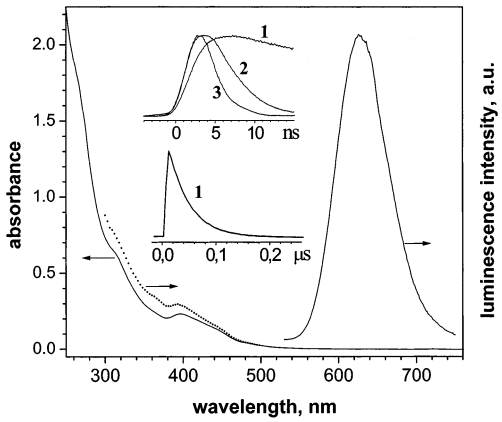


**Figure 3.** Optical absorption, luminescence excitation (dotted line, $\lambda_{em}$ = 620 nm), and emission ($\lambda_{exc}$ = 400 nm) spectra of $Au_{18}Se_8$ complex **I** in dichloromethane at room temperature. The inserts show a delayed rise and a decay of the luminescence of **I** in Ar-purged dichloromethane (**1**) compared with the fluorescence of Rhodamine B in methanol (**2**), both excited with a $N_2$-laser pulse at 337 nm (**3**) and recorded at 620 nm.

A combination of an integrating sphere with a cryostat for quantitative measurements of PL at low temperatures is technically challenging.[26] In this work, PL of polycrystalline powders of **I** and **II** (in the sealed glass capillaries) was measured at 77 K in a simple liquid nitrogen optical cell. The quantum yield was estimated by comparing the PL at 77 and 293 K in the same geometry, assuming a similar angular distribution of the light emission at both temperatures. Close values of $\varphi_{PL}$ at 77 K obtained by collecting PL at different angles (~30° and 90°) with respect to the excitation beam support this assumption.

## 3. Results and Discussion

**3.1. Absorption Spectra.** The gold selenide complexes **I**−**IV** (Figure 1) are soluble in dichloromethane up to ~$10^{-3}$ M, forming yellow solutions. The absorption spectrum of **I** shows a visible onset near ~470 nm (2.63 eV), a broad band at 397 nm ($\epsilon$ = 23000 $M^{-1}cm^{-1}$), and a steep increase below 300 nm likely due to the absorption of the ligands (Figure 3). In concentrated solutions a weak absorption of **I** is seen up to ~600 nm. The complex **II** shows a relatively featureless absorption curve starting at ~500 nm (Figure 7). The extinction coefficient at a ~380 nm shoulder is 2100 $M^{-1}$ $cm^{-1}$, i.e., the near-UV absorption arising from the $Au_{10}Se_4$-core **II** is much weaker compared to the $Au_{18}Se_8$-core **I**. Similar poorly structured spectra with onsets at ~500 nm are also observed for **III** and **IV** (not shown). The absorption edges of polycrystalline powders of **I** and **II** estimated at ~630 and ~530 nm, respectively, correspond roughly to those in the concentrated solutions.

**3.2. Visible Photoluminescence of the $Au_{18}Se_8$ Complex I.** Under UV−visible irradiation (300−500 nm) **I** emits red PL which is particularly bright in the solid state. The spectra of PL are shown in Figures 3 and 4. The emission maxima, lifetimes and quantum yields of PL are listed in Table 1.

The emission of **I** in dichloromethane at room temperature has a maximum at 628 nm (1.97 eV). The excitation spectrum corresponds well to the absorption profile (Figure 3). The quantum yield of PL is moderate: $2.4 \times 10^{-3}$ in argon-purged $CH_2Cl_2$. According to kinetic measurements, this PL rises up within ~2 ns with regard to the laser excitation pulse and then decays monoexponentially with $\tau_{PL}$ = 63 ns (Figure 3, inserts). Dissolved molecular oxygen efficiently quenches the luminescence: in oxygen-purged $CH_2Cl_2$, $\tau_{PL}$ and $\varphi_{PL}$ decrease to 15 ns and $6 \times 10^{-4}$, respectively. Taking the oxygen concentration as ~$1 \times 10^{-2}$ M,[27] this corresponds to the bimolecular quenching rate constant of ~$5 \times 10^9$ $M^{-1}$ $s^{-1}$, i.e., similar to the typical rate constants of oxygen quenching of triplet aromatic molecules.[28] The $Au_{18}Se_8$ complex is scarcely soluble in *N*,*N*-DMF and in this solvent shows PL properties similar to those in $CH_2Cl_2$ (Table 1).

Photoluminescence of the solid polycrystalline complex **I** with a maximum at 629 nm is very close to that in the solution (Figure 4 ), but significantly stronger ($\varphi_{PL}$ = 0.075). In fact, due to this PL the solid **I** gains a bright-orange-red color. By cooling **I** down to 77 K the emission spectrum shifts slightly to 618 nm and becomes more narrow (Figure 4). Furthermore, $\varphi_{PL}$ increases smoothly up to ~0.8 at 77 K. It is one of the highest PL efficiencies so far reported for gold complexes.[10] As in the solution, the rise of PL is delayed by ~2 ns relative to the laser excitation pulse. The decay of PL of the solid **I** occurs on a microsecond time scale and can be fitted with a biexponential curve (Table 1; Figure 4, inserts).

The independence of PL on the excitation wavelength, delayed rise, and radiative lifetime ($\tau_{rad} = \tau_{PL}/\varphi_{PL}$) of ~20 $\mu$s suggests that PL occurs from a relaxed excited state of a triplet character, i.e., PL of **I** can be considered as phosphorescence. This state is denoted as T in the simplified model of photophysical processes in Figure 5. In this model photoexcitation into higher excited singlet-like states $S_n$ of **I** is followed by rapid relaxation to the lowest excited state of a singlet character, $S_1$. Intersystem conversion into T occurs within ~2 ns. The rate of the radiative decay of T to $S_0$, $k_{rad} = 1/\tau_{rad}$, remains roughly constant both in the solid state at different temperatures and in fluid solution, whereas the rate of nonradiative decay, $k_{nr}$, changes dramatically, being the highest in solution and resulting in the low value of $\varphi_{PL}$ (Figure 5). One should note that although this singlet−triplet-state model "borrowed" from organic photochemistry describes well the photophysical properties of **I**, it is only an approximation because of significant relativistic effects in gold compounds.[15]

It is tempting to attribute the remarkable photophysical properties of $Au_{18}Se_8$ complex **I** such as the bright PL in the solid state, large absorption coefficient, small shift of PL, and high photostability in solution (see below) to the peculiar "multishell" and "rigid" structure of its gold selenide core. In this respect, a comparison with similar structures would be helpful. However, selective synthesis of the structurally related polynuclear gold complexes, having, for instance, an additional AuSe shell or other ligands, remains a great challenge. Recently, Yam et al.[29] have prepared a gold(I)−sulfido complex $[Au_6S_2(Ph_2PN(p\text{-}CH_3C_6H_4)PPh_2)_3](ClO_4)_2$, whose $Au_6S_2$ core corresponds to the inner $Au_6Se_2$ cube of **I** (Figure 1). Similar to **I**, the $Au_6S_2$ complex shows an intense PL at ~630 nm in the solid state with a microsecond decay. However, in dichloromethane the PL is dramatically shifted to ~810 nm. The shift has been attributed to large structural distortions of the excited complex in fluid solution. In difference to the $Au_6S_2$ complex, large structural distortions of **I** are hardly allowed. Also known is the $[Au_{18}S_8(dppe)_6]^{2+}$ complex synthesized by Bates and Waters as early as in 1987,[30] which seems to be a full structural analogue of **I**. Unfortunately, the photophysical properties of this $Au_{18}S_8$ complex have not been investigated so far.

**3.3. Photosensitization of Singlet Oxygen.** Quenching of the photoexcited complex **I** in solution by dissolved molecular oxygen produces singlet oxygen, $^1O_2$, as evidenced by its characteristic narrow emission band at ~1275 nm (Figure 6).[31] The quantum yield of $^1O_2$ is 0.17 ± 0.02 in oxygen-saturated $CH_2Cl_2$ and independent of the excitation wavelength (300−

**TABLE 1: Photoluminescence Properties of the Gold Selenide Complexes I and II**

| | $T$ (K) | $\lambda_{em}$ (nm) | $\varphi_{PL}$[a] | $\tau$[b] |
|---|---|---|---|---|
| complex **I**: | | | | |
| in dichloromethane | 293 | 628 | $2.4 \times 10^{-3}/6 \times 10^{-4}$[c] | 63 ns/15 ns[c] |
| in *N*,*N*-dimethylformamide | 293 | 631 | | 43 ns/10 ns[c] |
| polycrystalline powder | 293 | 629 | 0.075 | 180 ns (40%); 1.13 $\mu$s (60%)[d] |
| polycrystalline powder | 77 | 618 | ~0.8 | 2.3 $\mu$s (26%), 12.2 $\mu$s (74%)[d] |
| complex **II**: | | | | |
| in dichloromethane | 293 | 880 | $(4 \pm 1) \times 10^{-3}$ | 21−38 ns, 120−180 ns, 0.37−2 $\mu$s[e] |
| polycrystalline powder | 293 | ~970 | $(3.5 \pm 1) \times 10^{-4}$ | 8 ns; 85 ns[d,f] |
| polycrystalline powder | 77 | ~1020 | $\sim 3 \times 10^{-3}$ | 300 ns; 2 $\mu$s[d,f] |

[a] Emission quantum yield; $\lambda_{exc} = 400$ nm; estimated error ±15% when not stated otherwise. [b] Luminescence lifetime determined from exponential fits of the luminescence decay curve; pulse excitation with a $N_2$-laser at 337 nm. [c] In Ar-purged/$O_2$-purged solutions. [d] Biexponential fit. [e] Three exponential fit; decay kinetics depends on the emission wavelength. [f] The ratio between exponential components depends on the emission wavelength.

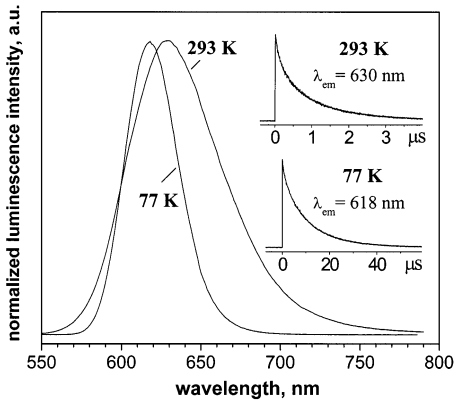


**Figure 4.** Luminescence emission spectra of the polycrystalline $Au_{18}Se_8$ complex **I** at 293 and 77 K. The inserts show a decay of the luminescence excited by a $N_2$-laser at 337 nm.

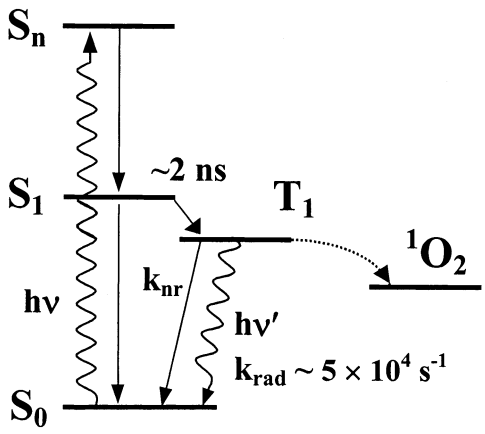


**Figure 5.** Energy diagram for the $Au_{18}Se_8$ complex **I**. Photoexcitation into higher excited singlet-like electronic states $S_n$ is followed by rapid relaxation to $S_1$ (~2.6 eV). Intersystem conversion into the excited triplet-like state $T_1$ (~2.0 eV) occurs within ~2 ns both in the solid state and in solution. In contrast to nonradiative relaxation of $T_1$, $k_{nr}$, the rate of radiative relaxation, $k_{rad}$, is similar in the solid state at different temperatures and in fluid solution (see Results and Discussion). Another decay channel for $T_1$ in solution is sensitization of singlet oxygen, $^1O_2$. Energies of $S_1$ and $T_1$ are estimated from the absorption and emission spectra of **I**, respectively.

500 nm) within experimental error. Taking into account the intrinsic lifetime of PL and that of the quenched PL (Table 1), one can estimate that at least ~22% of the quenching collisions of photoexcited **I** with dissolved oxygen result in the formation of $^1O_2$. Such efficiency and a linear dependence of the $^1O_2$ signal on the excitation intensity suggest energy transfer from an excited state of the $Au_{18}Se_8$ complex to molecular oxygen as a mechanism of the formation of $^1O_2$.[32] The effective sensitization

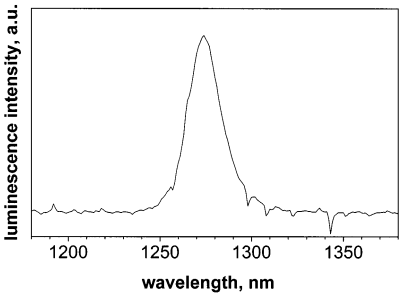


**Figure 6.** Infrared luminescence of singlet oxygen photosensitized by the $Au_{18}Se_8$ complex **I** in air-equilibrated dichloromethane ($\lambda_{exc} = 350$ nm, emission slit width 5 nm).

of $^1O_2$ supports a triplet character of the luminescent state T of **I**. Evidently, the quantum yield of T, $\varphi_T$, should be at least the same as the efficiency of $^1O_2$ formation in the quenching collisions with $O_2$, i.e., $\varphi_T \geq 0.22$ in dichloromethane.

These results appear to be the first experimental evidence of a relatively efficient photosensitization of singlet oxygen by a gold complex. Quenching of triplet excited states by oxygen with a generation of $^1O_2$ is a common process in organic photochemistry,[32] it has also been well documented for metalloporphyrins[33] and diimine complexes of ruthenium and osmium,[34] but very little data is available for other metal complexes. It is not clear at the moment, which factors determine that the $Au_{18}Se_8$ complex **I** efficiently photosensitizes singlet oxygen, whereas the $Au_{10}Se_4$ complex **II**, as probably the majority of other luminescent gold complexes with relatively long-lived excited states,[10] does not (see below). Another exception may be $[Au_3(dmmp)_2](ClO_4)_3$ [dmmp = bis(dimethylphosphinomethyl) methylphosphine]. A photooxidative cleavage of DNA by this trinuclear gold complex in air-saturated aqueous solutions was demonstrated and attributed to the intermediacy of superoxide radical, but photosensitization of singlet oxygen was not ruled out.[35]

**3.4. Near-Infrared Photoluminescence of the $Au_{10}Se_4$ Complex II.** Under UV−visible irradiation (300−500 nm) the complex **II** emits no visible luminescence, but a broad near-infrared PL with a maximum up to ~1020 nm in the solid state at 77 K. To our knowledge, such a low-energy emission (~1.2 eV) and a large Stokes shift have not yet been reported for gold compounds. The spectra of PL are shown in Figures7 and 8. The emission maxima, lifetimes, and quantum yields are listed in Table 1.

Many features of the photoluminescence of **II** differ dramatically from those of **I**. The maximum of the relatively broad emission spectrum of **II** shifts strongly from 880 nm in dichloromethane solutions up to ~970 nm in the solid state at room temperature and to ~1020 nm at 77 K (Figures 7 and 8).

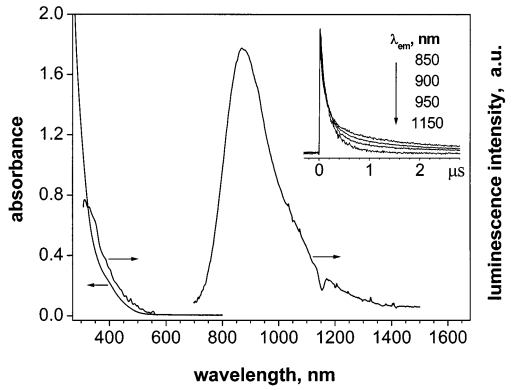


**Figure 7.** Optical absorption, luminescence excitation (dotted line, $\lambda_{em}$ = 920 nm) and emission ($\lambda_{exc}$ = 400 nm) spectra of the $Au_{10}Se_4$ complex **II** in dichloromethane. A dip on the luminescence curve at 1150 nm is due to the solvent absorption. The insert shows normalized luminescence decay curves at different emission wavelengths (initial parts of the decay curves are shown for clarity; pulse excitation with a $N_2$-laser at 337 nm).

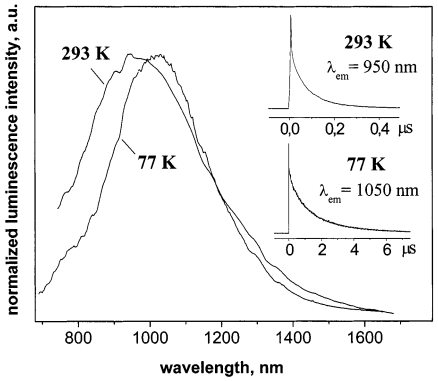


**Figure 8.** Luminescence emission spectra of the polycrystalline $Au_{10}Se_4$ complex **II** at 293 and 77 K ($\lambda_{exc}$ = 400 nm). The inserts show luminescence decay curves recorded at 950 and 1050 nm, respectively, after pulse excitation with a $N_2$-laser at 337 nm.

On the other hand, the quantum yield of PL changes relatively moderately from $(4 \pm 1) \times 10^{-3}$ in $CH_2Cl_2$ to $(3.5 \pm 1) \times 10^{-4}$ and $\sim 3 \times 10^{-3}$ in the solid state at 293 and 77 K. The excitation spectrum of PL in solution does not follow the steep increase of absorption below ~350 nm (Figure 7), suggesting nonradiative relaxation of the electronic states of **II** excited at the short wavelengths. These states are probably localized on the phosphine ligands. In the case of **I**, the absorption due to the "core-related" electronic transitions appears to be much larger than in **II** (see Section 3.1), which may result in a relatively small contribution of the "ligand-localized" excited states in the absorption and PL excitation spectra of **I** down to ~300 nm. Another remarkable feature of **II** is a complicated multiexponential luminescence decay kinetics, in particular in solution, which depends on the emission wavelength (Figures 7 and 8, and Table 1). The PL decay in solution and in the solid state at 77 K is dominated by microsecond components, whereas the decay in the solid state at room temperature occurs within tens of nanoseconds. Similarly to **I**, the faster relaxation of the luminescent excited state(s) of **II** results in the lower quantum yield of PL. Finally, in contrast to **I**, molecular oxygen does not influence notably the luminescence intensity and kinetics of **II** in solution.

The most unusual property of the $Au_{10}Se_4$ complex **II** is its near-infrared luminescence. Whetten et al. reported a weak PL at ~1100−1600 nm from metallic Au clusters with ~38−145 gold atoms.[7] But for gold complexes, the near-infrared spectral region practically has not been explored so far. The complexes with a few gold atoms emit typically in the visible spectral range (~450−700 nm). This emission is usually assigned to triplet ligand-to-metal or metal-to-ligand (depending on the nature of ligands) charge-transfer electronic configurations mixed with ds/dp states localized on neighboring (interacting) gold atoms.[10] In their theoretical study of binuclear gold complexes with bridging phosphines Zhang and Che found that their emission can be substantially red-shifted due to interaction of a corresponding excited state with solvent molecules.[36] However, witihin these models it is hard to explain the origin of the very low energy emission of **II** having the maximum at ~1020 nm and tailing up to ~1500 nm in the solid state at 77 K (Figure 8). This requires further experimental and theoretical study.

The large Stokes shift and microsecond decay components suggest formally a triplet character of the luminescent excited electronic state(s) of **II**. However, a simplified photophysical model applied to the complex **I** (Figure 5) cannot adequately describe many features of the PL of **II**, for instance, the wavelength-dependent luminescence decay in solution. Compared to **I**, the $Au_{10}Se_4$ core **II** stabilized by the "loose" bis-(diphenylphosphanyl)pentane ligands seems to be a much more flexible structure (Figure 1). Therefore we suppose that the complex **II** can thermally sample many varied configurations in the ground as well as in excited electronic states, especially in solution. Small differences between these configurations may result in significant changes of the gold−gold interactions and, correspondingly, of the photoluminescence properties. The averaged contributions of many configurations (excited electronic states) observed in the experiment may explain the multiexponential wavelength-dependent PL kinetics. Another explanation might also be aggregation of molecules of **II** in solution, resulting in manifold of oligomeric species with different PL properties.[37] However, filtration (0.2 $\mu$m PTFE-filter) and dilution (~$10^{-5}$ M) of solutions of **II** had no significant effect on its absorption and PL. Further study is required to clarify the complicated photodynamics of this complex.

The $Au_{10}Se_4$ complexes **III** and **IV** (Figure 1) can be considered as the "isomers" of **II** with regard to the same composition of the gold selenide cores. Furthermore, these complexes are also stabilized with the phosphine ligands and therefore show similar gold−phosphor bonding between the core and the ligand shell. However, in difference to **II**, no significant PL was observed in dichloromethane solutions of **III** and **IV**. Namely, a light emission around ~800 and 460 nm was registered for **III** and **IV**, respectively, but its intensity was very weak with an estimated quantum yield of $<10^{-5}$ for both complexes. These results suggest again that the configuration of the $Au_{10}Se_4$ core is crucial for the photoluminescence properties.

The quantum efficiency of the near-infrared PL of **II** is quite moderate, but, in fact, comparable to the fluorescence quantum yields of typical organic laser dyes used in the near-infrared region. Indeed, it is well-known that $\varphi_{fluor}$ of the latter are far inferior compared to the laser dyes emitting in the UV−visible region ($\varphi_{fluor}$ up to ~1 in solution) because of the efficient vibrational relaxation of low-lying electronic excited states.[38] A dramatic decrease of $\varphi_{fluor}$ with the increasing emission wavelength is illustrated by Table 2, where absorption and emission maxima and fluorescence quantum yields for several organic laser dyes are listed. Keeping in mind a strong influence of the gold−gold interactions on the photophysical properties of polynuclear gold compounds, one can expect that a fine

**TABLE 2: Fluorescence Quantum Efficiency for Several Organic Laser Dyes with the Emission Wavelengths from the Visible to the Near-Infrared Region**

| laser dye/ solvent | $\lambda_{abs}$ (nm)[a] | $\lambda_{em}$ (nm)[a] | $\varphi_{PL}$ [b] |
|---|---|---|---|
| Rhodamine 6G/ methanol | 527 | 553 | 0.95 (532)[c] |
| Rhodamine 800/ methanol | 679 | 706 | $0.21 \pm 0.02$ (620) |
| Styryl 20/ propylencarbonate | 626 | 975 | $(8 \pm 2) \times 10^{-3}$ (625) |
| IR26/ dichloromethane | 1077 | 1128 | $(5 \pm 2) \times 10^{-4}$ (400); $\sim 1 \times 10^{-3}$ (970) |

[a] Absorption and fluorescence emission maxima. [b] Fluorescence quantum yields determined using Rhodamine 6G in methanol as a primary quantum yield reference; the excitation wavelengths are indicated in brackets. [c] Ref 22.

"tuning" of the structure of **II**, for example, by a (post)-modification of the ligands, may substantially improve the efficiency of its PL. We remark that the relationships between the structure and photophysical properties of gold complexes, especially of polynuclear ones, are poorly understood. Further synthetic work together with photophysical studies as well as progress in a theoretical modeling may lead to new gold−chalcogenide clusters with interesting infrared PL properties, for example, with a potential for infrared lasing.

**3.5. Photostability.** In parallel to its remarkable chemical stability,[20] the $Au_{18}Se_8$ complex **I** demonstrates a high photostability. No photodecomposition of this compound was observed during the experiments described above (see Experimental Details). In addition, we irradiated a $3 \times 10^{-5}$ $M^{-1}$ solution of **I** in $CH_2Cl_2$ for a few hours with a 200 mW Ar-ion laser beam at 476.5 nm. Significant changes in the absorption spectrum and a decrease of PL were observed only after absorption and dissipation of $\sim 2.5 \times 10^6$ kJ/mol excitation energy ($\sim 10^4$ photons per $Au_{18}Se_8$ unit) for both argon-purged and air-equilibrated solutions. A dark deposit appeared on the walls of a quartz cuvette where the laser beam crossed the solution. This may indicate a predominant photodecomposition of the adsorbed species. After the irradiation, within hours, a dark brown precipitate formed in the solution. According to scanning electron microscopy, it consisted of agglomerates of particles with sizes of ∼10−100 nm. An incorporated EDX element analysis found gold and selenium, but no phosphor. These results suggest a complicated photodecomposition of **I**, which is likely initiated by a detachment of the phosphine ligands followed by a "coalescence" of the gold selenide cores. The $Au_{10}Se_4$ complex **II** photodecomposes similarly with a formation of precipitate, but was found to be substantially less photostable than **I**.

## 4. Summary

The ligand-stabilized gold(I) selenide complexes $[Au_{18}Se_8(dppe)_6]Br_2$ **I** and $[Au_{10}Se_4(dpppe)_4]Br_2$ **II** (Figure 1) demonstrate novel and unusual photophysical properties for the class of organic gold compounds in general and cluster-like polynuclear gold−chalcogenide complexes in particular. These are the relatively efficient photosensitization of singlet oxygen by **I** in solution (the quantum yield of $^1O_2$ is 0.17 in $O_2$-saturated dichloromethane) and the low-energy, near-infrared luminescence of **II** excited with UV−visible light (PL maximum is at 880 and ∼1020 nm in a dichloromethane solution and in the solid state at 77 K, respectively).

Beside the photosensitization of singlet oxygen, **I** is distinguished by the bright-red long-lived photoluminescence in the solid state ($\varphi_{PL} \sim 0.8$ at 77 K), large absorption coefficient, and high photo and chemical stability. All these remarkable features are likely related to the particular compact "multishell" structure of the $Au_{18}Se_8$ core. In solution, the luminescence of **I** is weak because of the fast nonradiative decay (within tens of nanoseconds) of the corresponding excited state of a triplet character. The effective sensitization of singlet oxygen occurs due to a fast, diffusion-limited quenching of this state by molecular oxygen.

The quantum efficiency of the near-infrared PL of **II** is quite moderate (ca. 0.4% both in fluid solution and in the solid state at 77 K). It is nevertheless comparable to a typical fluorescence quantum yield of organic near-infrared fluorophors such as laser dyes Styryl-20 and IR26. The structure of the $Au_{10}Se_4$ core appears to be crucial for the near-infrared PL: the "isomeric" $Au_{10}Se_4$ complexes $[Au_{10}Se_4(dppm)_4]Br_2$ **III** and $[Au_{10}Se_4(depe)_4]Cl_2$ **IV** (Figure 1) show no significant PL. One can assume that the efficiency and emission spectrum of the near-infrared PL may be dramatically changed by "adjusting" the structure of the $Au_{10}Se_4$ core **II**.

In this work we have not attempted to assign the luminescent excited electronic states of **I** and **II** to specific configurations such as mixed ligand-to-metal charge transfer/metal-localized states which have usually been suggested for luminescent gold complexes with phosphine ligands.[10] A detailed quantum chemical study is necessary for such assignment and explanation of the origin of the unusual near-infrared PL of **II** as well as for a general qualitative understanding of the relative effects of gold−ligand bonding and gold−gold interactions on the optical properties of polynuclear gold complexes such as **I** and **II**. DFT calculations of the electronically excited states and dipole oscillator strengths of several model gold selenide structures including **II** are in progress and will be presented elsewhere.[39]

Finally, we note that, in terms of size, the large polynuclear gold−chalcogenide complexes are comparable to small metallic gold clusters with ∼20−40 gold atoms stabilized by an adsorbate (typically thiol) shell.[3] Furthermore, these ∼1.1−1.7 nm metallic clusters (∼38−145 gold atoms) were found to show a weak near-infrared PL in the range of ∼1100−1600 nm.[7] Taken together with our results it appears that near-infrared luminescence can occur in very different classes of nanometer-size gold structures.

**Acknowledgment.** This work was supported by the Deutsche Forschungsgemeinschaft (SFB 195). The authors are grateful to Dr. S. Malik (Forschungszentrum Kalrsruhe, INT) for the SEM analysis.

## References and Notes

(1) *Handbook of Nanostructured Materials and Nanotechnology*; Nalwa, H. S., Ed.; Academic Press: San Diego, 2000; Vol. 4.

(2) Murray C. B.; Norris, D. J.; Bawendi, M. G. *J. Am. Chem. Soc.* **1993**, *115*, 8706; Empedocles, S. A.; Neuhauser, R.; Shimizu, K.; Bawendi, M. G. *Adv. Mater.* **1999**, *11*, 1243; Rogach, A. L.; Kornowski, A.; Gao, M. Y.; Eychmuller, A.; Weller, H. *J. Phys. Chem. B* **1999**, *103*, 3065.

(3) Brust, M.; Fink, J.; Bethell, D.; Schiffrin, D. J.; Kiely, C. *J. Chem. Soc. Chem. Commun.* **1995**, 1655; Schaaff, T. G.; Whetten, R. L. *J. Phys. Chem. B* **2000**, *104*, 2630; Omary, M. A.; Rawadeshdeh-Omary, M. A.; Chusuei, C. C.; Fackler, J. P.; Bagus, P. S. *J. Chem. Phys.* **2001**, *114*, 10695.

(4) Talapin, D. V.; Rogach, A. L.; Kornowski, A.; Haase, M.; Weller, H. *Nano Lett.* **2001**, *1*, 207.

(5) Alivisatos, A. P. *Science* **1996**, *271*, 933.

(6) Soloviev, V. N.; Eichhöfer, A.; Fenske, D.; Banin, U. *J. Am. Chem. Soc*. **2001**, *123*, 2354.
(7) Bigioni, T. P.; Whetten, R. L.; Dag, Ö. *J. Phys. Chem. B* **2000**, *104*, 6983.
(8) Mohamed, M.B.; Volkov, V.; Link, S.; El-Sayed, M. A. *Chem. Phys. Lett*. **2000**, *317*, 517.
(9) Huang, T.; Murray, R. W. *J. Phys. Chem. B* **2001**, *105*, 12498.
(10) For a review see, for example, Schmidbaur, H. *Chem. Soc. Rev*. **1995**, 391; Yam, V. W.-W.; Lo, K. K.-W. *Chem. Soc. Rev*. **1999**, *28*, 323; Vogler, A.; Kunkely, H. *Coord. Chem. Rev*. **2001**, *219*−*221*, 489.
(11) Mansour, M. A.; Connick, W. B.; Lachicotte, R. J.; Gysling, H. J.; Eisenberg, R. *J. Am. Chem. Soc*. **1998**, *120*, 1329.
(12) Yam, V. W.-W.; Li, C.-K.; Chan, C.-L. *Angew. Chem., Int. Ed. Engl*. **1998**, *37*, 2857; Yam, V. W.-W.; Chan, C. L.; Li, C. K.; Wong, K. M. C. *Coord. Chem. Rev*. **2001**, *216*, 173.
(13) Kittel, C. *Introduction to Solid State Physics*, 5th ed.; Wiley: New York; 1976; p 32, Table 5.
(14) Gilb, S.; Weis, P.; Furche, F.; Ahlrichs, R.; Kappes, M. M. *J. Chem. Phys*. **2002**, *116*, 4094.
(15) Pyykkö, P. *Chem. Rev*. **1997**, *97*, 597.
(16) King, C.; Wang, J.-C.; Khan, M. N. I.; Fackler, J. P., Jr. *Inorg. Chem*. **1989**, *28*, 2145.
(17) Forward, J. M.; Bohmann, D.; Fackler, J. P., Jr.; Staples, R. J. *Inorg. Chem*. **1995**, *34*, 6330.
(18) van Zyl, W. E.; López-de-Luzuriaga, J. M.; Fackler, J. P., Jr. *J. Mol. Struct.* **2000**, *516*, 99.
(19) Yam, V. W.-W.; Cheng, E. C.-C.; Cheung, K.-K. *Angew. Chem., Int. Ed. Engl*. **1999**, *38*, 197; Yam, V. W.-W.; Cheng, E. C.-C.; Zhou, Z.-Y. *Angew. Chem., Int. Ed. Engl*. **2000**, *39*, 1683.
(20) Fenske, D.; Langetepe, T.; Kappes, M. M.; Hampe, O.; Weis, P. *Angew. Chem., Int. Ed. Engl*. **2000**, *39*, 1857.
(21) Langetepe, T. Ph.D. Thesis, University Karlsruhe, 2001; Langetepe, T.; Sevillano, P.; Fenske, D. In preparation.
(22) Bindhu, C. V.; Harilal, S. S.; Nampoori, V. P. N.; Vallabhan, C. P. G. *Mod. Phys. Lett*. **1999**, *B13*, 563.
(23) Shimizu, O.; Watanabe, J.; Imakubo, K.; Naito, S. *Chem. Lett*. **1999**, 67.
(24) Arbogast, J. W.; Foote, C. S. *J. Am. Chem. Soc*. **1991**, *113*, 8886.
(25) Wrighton, M. S.; Ginley, D. S.; Morse, D. L. *J. Phys. Chem*. **1974**, *78*, 2229; Ferreira, L. F. V.; Freixo, M. R.; Garcia, A. R. *J. Chem. Soc., Faraday Trans*. **1992**, *88*, 15.
(26) Westphäling, R.; Ullrich, P.; Hoffmann, J.; Kalt, H.; Klingshirn, C.; Ohkawa, K.; Hommel, D. *J. Appl. Phys*. **1998**, *84*, 6871; Mei, P.; Murgia, M.; Taliani, C.; Lunedei, E.; Muccini, M. *J. Appl. Phys*. **2000**, *88*, 5158.
(27) *Solubilities of Inorganic and Organic Compounds*; Stephen, H., Stephen, T., Eds.; Pergamon Press: Oxford, 1963; Vol. 1, p 575.
(28) Abdel-Shafi, A. A.; Wilkinson, F. *J. Phys. Chem. A* **2000**, *104*, 5747; Abdel-Shafi, A. A.; Worall, D. R.; Wilkinson, F. *J. Photochem. Photobiol. A* **2001**, *142*, 133; and references therein.
(29) Yam, V. W.-W.; Cheng, E. C.-C.; Zhu, N. *Angew. Chem., Int. Ed. Engl*. **2001**, *40*, 1763.
(30) Bates, P. A.; Waters, J. M. *Acta Crystallogr. Sect. A* **1987**, *43*, C194.
(31) Ogilby, P. R. *Acc. Chem. Res*. **1999**, *32*, 512.
(32) Foote, C. S.; Clennan, E. L. In *Active Oxygen in Chemistry*; Foote, C. S., Valentine, J. S., Greenberg, A., Liebman, J. F., Eds.; Chapman and Hall: London, 1995; p 105.
(33) Bonnett, R. *Chem. Soc. Rev*. **1995**, 19.
(34) Demas, J. N.; McBride, R. P.; Harris, E. W. *J. Am. Chem. Soc*. **1977**, *99*, 3547; Abdel-Shafi, A. A.; Beer, P. D.; Mortimer, R. J.; Wilkinson, F. *J. Phys. Chem. A* **2000**, *104*, 192, and references therein.
(35) Yam, V. W.-W.; Choi, S. W.-K.; Lo, K. K.-W.; Dung, W.-F.; Kong, R. Y.-C. *J. Chem. Soc. Chem. Commun*. **1994**, 2379.
(36) Zhang, H.-X.; Che, C.-M. *Chem. Eur. J*. **2001**, *7*, 4887.
(37) Rawashdeh-Omary, M. A.; Omary, M. A.; Patterson, H. H.; Fackler, J. P. *J. Am. Chem. Soc*. **2001**, *123*, 11237.
(38) Elsaesser, T.; Kaiser, W. In *Topics in Applied Physics, Vol. 70, Dye Lasers: 25 Years*; Stuke, M., Ed.; Springer-Verlag: Berlin, Heidelberg; p 95.
(39) Ahlrichs, R. Private communication.